JACS
JOURNAL OF THE AMERICAN CHEMICAL SOCIETY
pubs.acs.org/JACS
Article

A *N*-Phosphinoamidinato NHC-Diborene Catalyst for Hydroboration

Jun Fan, Jian-Qiang Mah, Ming-Chung Yang, Ming-Der Su,* and Cheuk-Wai So*

Cite This: *J. Am. Chem. Soc.* 2021, 143, 4993−5002
Read Online

ABSTRACT: The use of the *N*-phosphinoamidinato NHC-diborene catalyst **2** for hydroboration is described. The *N*-phosphinoamidine $tBu_2PN(H)C(Ph)=N(2,6\text{-}iPr_2C_6H_3)$ was reacted with *n*BuLi in Et_2O to afford the lithium derivative, which was then treated with $B_2Br_4(SMe_2)_2$ in toluene to form the *N*-phosphinoamidinate-bridged diborane **1**. It was reacted with the N-heterocyclic carbene IMe $(:C\{N(CH_3)C(CH_3)\}_2)$ and excess potassium graphite at room temperature in toluene to give the *N*-phosphinoamidinato NHC-diborene compound **2**. It can stoichiometrically activate ammonia−borane and carbon dioxide. It also showed catalytic capability. A 2 mol % portion of **2** catalyzed the hydroboration of carbon dioxide (CO_2) with pinacolborane (HBpin) in deuterated benzene (C_6D_6) at 110 °C (conversion >99%), which afforded the methoxyborane [pinBOMe] (yield 97.8%, TOF 33.3 h^{-1}) and the bis(boryl) oxide $[(pinB)_2O]$. In addition, 5 mol % of **2** catalyzed the N-formylation of secondary and primary amines by carbon dioxide and pinacolborane to yield the N-formamides (average yield 91.6%, TOF 25.9 h^{-1}). Moreover, **2** showed chemoselectivity toward catalytic hydroboration of carbonyl compounds. In mechanistic studies, the B=B double bond in compound **2** activated the substrates, the intermediates of which then underwent hydroboration with pinacolborane to yield the products and regenerate catalyst **2**.

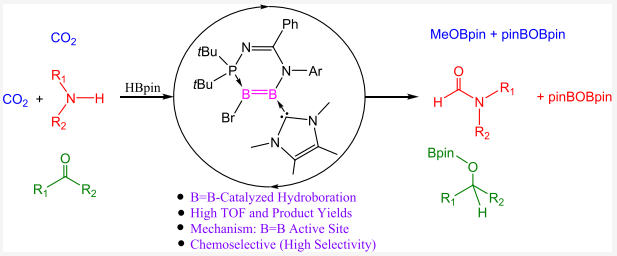

INTRODUCTION

Multiply bonded main-group compounds containing an E=E double-bond (E = main-group element) or E≡E triple bond are of particular interest, as they exhibit transition-metal-like reactivity to activate and functionalize small molecules due to the possession of a HOMO and LUMO with a small energy difference.[1] As an illustration, stable diboryne, diborene, dialumene, disilene, digermyne, and distannyne were capable of noncatalytically activating a diversity of small molecules: namely, dihydrogen, ammonia, nitrous oxide, carbon monoxide, and carbon dioxide.[2−4] However, reversible activation is scarcely found, whereby only the distannyne $[Ar^{iPr}SnSnAr^{iPr}]$ (Ar^{iPr} = C_6H_3-2,6-Ar_2, Ar = 2,6-$iPr_2C_6H_3$) reversibly underwent cycloaddition with ethylene and norbornadiene,[5] in addition to the reversible oxidation with H_2.[6] These results indicate that small molecules have difficulty in dissociating from the main-group-element centers after activation. As such, catalytic organic transformations mediated by multiply bonded main-group compounds are rare, with only two examples being reported. The first example was the digermyne-catalyzed cyclotrimerization of terminal alkynes, where the digermyne [TbbGeGeTbb] (Tbb = 4-*t*Bu-2,6-$[CH(TMS)_2]C_6H_2$, TMS = $SiMe_3$) was a precatalyst (Figure 1) that reacted with the alkyne to afford the digermabenzene.[7] It acted as the active catalyst to react with three more molecules of alkynes to form 1,2,4-triarylbenzene with high regioselectivity. The second example was a dialumene-catalyzed CO_2 hydroboration, where the NHC-dialumene $[(IPrMe)(tBu_2MeSi)AlAl(SiMetBu_2)\text{-}(IPrMe)]$ (IPrMe = $:C\{N(iPr)_2C(Me)\}_2$) was a precatalyst, which reacted with CO_2 to form a $Al(\mu\text{-}CO_3)(\mu\text{-}O)Al$ six-membered ring.[8] This acted as the active catalyst to react with HBpin and CO_2 to form formoxyborane. In these catalyses, the Al=Al and Ge≡Ge multiple bonds were not able to be regenerated after the catalytic cycle. These results give rise to the question of whether main-group multiple bonds can be involved in a catalytic cycle.

To prove the concept, we were interested in synthesizing a main-group-element multiply bonded delocalized compound for catalytic organic reactions, because the delocalization effect could facilitate restoration of the main-group-element multiple bond after a catalytic cycle. In this article, we report the synthesis of a *N*-phosphinoamidinato N-heterocyclic carbene-diborene catalyst and its application toward the catalytic hydroboration of carbon dioxide and catalytic N-formylation reactions of secondary and primary amines by carbon dioxide and pinacolborane, as well as the chemoselective catalytic hydroboration of carbonyl compounds. DFT calculations are also reported to rationalize our experimental findings.

Received: December 4, 2020
Published: January 15, 2021

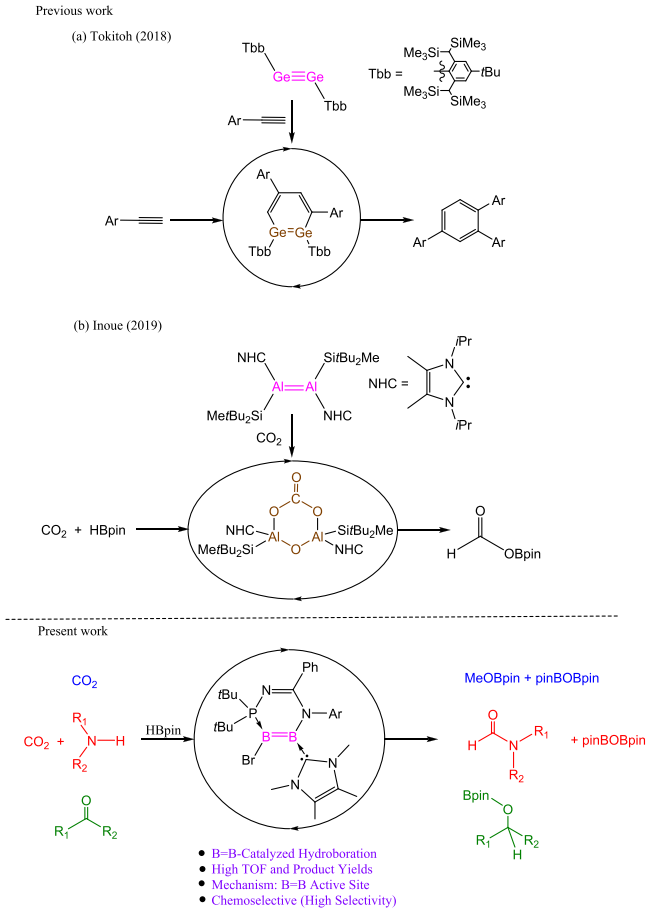

Figure 1. Multiply bonded main-group compounds for catalytic organic reactions.

RESULTS AND DISCUSSION

To begin with, the *N*-phosphinoamidine[9] was reacted with *n*BuLi in Et_2O for 3 h to afford the lithium derivative, which was then reacted with $B_2Br_4(SMe_2)_2$[10] in toluene for 12 h (Scheme 1). The LiBr that formed in the reaction mixture was

Scheme 1. Synthesis of 2

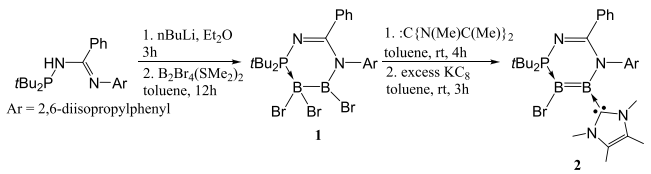

separated by filtration. After that, the filtrate was concentrated to afford the *N*-phosphinoamidinate-bridged diborane **1** as colorless crystals. The $^{11}B\{^1H\}$ NMR spectrum shows two signals at 55.5 and −11.9 ppm for sp^2 and sp^3 boron centers, respectively. The $^{31}P\{^1H\}$ NMR spectrum shows one signal at 35.9 ppm. X-ray crystallography of **1** shows that the ligand is bridging between two boron centers, where the length of the B1−B2 bond is 1.704(5) Å (Figure 2). Moreover, the length of the N1−B1 bond is 1.428(5) Å, indicating that the N1 lone pair of electrons delocalize to the vacant p orbital of the B1 center more than to the amidinate N1−C13−N2 skeleton (C13−N2 1.279(4) Å, C13−N1 1.423(4) Å).

Compound **1** was reacted with IMe (:C{N(CH_3)C(CH_3)}$_2$) at room temperature in toluene for 4 h to yield a

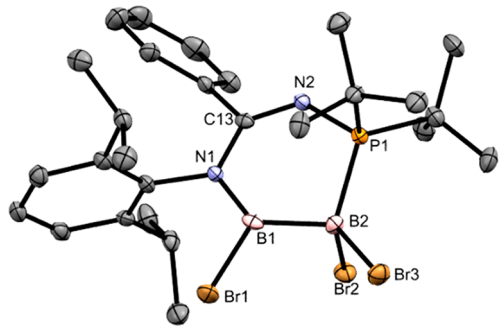

Figure 2. Molecular structure of **1** obtained by X-ray crystallography. Thermal ellipsoids are set at the 50% probability level. All hydrogen atoms are deleted for clarity. Selected bond lengths (Å) and angles (deg): B1−B2 1.704(5), P1−B2 1.940(4), N1−B1 1.428(5), N1−C13 1.423(4), N2−C13 1.279(4), P1−N2 1.673(3), N1−B1−B2 124.3(3), B1−B2−P1 103.9(2), B2−P1−N2 104.53(15), P1−N2−C13 127.8(2), N2−C13−N1 126.3(3), C13−N1−B1 120.8(3).

red precipitate, which was then reacted with excess KC_8 in toluene for 3 h at room temperature to yield a purple-red mixture (Scheme 1). The precipitate (graphite and KBr) that formed in the reaction mixture was removed by filtration. After that, the filtrate was concentrated to afford the phosphinoamidinato NHC-diborene compound **2** as a red crystalline solid. The $^{11}B\{^1H\}$ NMR spectroscopy displays two signals at 28.8 and 10.5 ppm, indicating that compound **2** is composed of a highly polarized B═B double bond. The signals are in the range of the ^{11}B NMR signals (12−32 ppm) of similar Lewis base-diborene complexes.[11−25] The $^{31}P\{^1H\}$ NMR signal (45.9 ppm) is shifted downfield in comparison with that of **1**. The $^{13}C\{^1H\}$ NMR signal at 152.9 ppm is attributable to the $C_{carbene}$ center coordinating with the boron atom. The molecular structure of compound **2** obtained by X-ray crystallography is composed of a planar boron-containing six-membered ring with a N2−C1−N1−B2 torsion angle of −0.07° (Figure 3). This indicates that there is six-π-electron delocalization along the N2−C1−N1−B1−B2 skeleton. The N1 lone pair electrons delocalize along the amidinate skeleton,

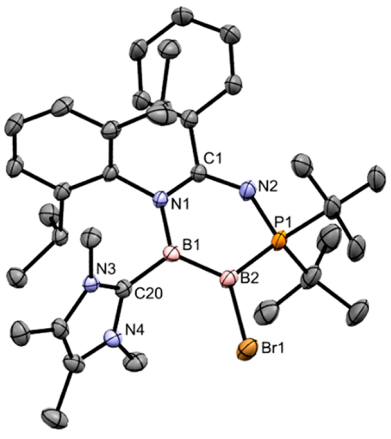

Figure 3. Molecular structure of **2** obtained by X-ray crystallography. Thermal ellipsoids are shown at the 50% probability level. All hydrogen atoms are removed for clarity. Selected bond lengths (Å) and angles (deg): B2−B1 1.562(4), P1−B2 1.851(4), N1−B1 1.526(4), N2−P1 1.641(2), C1−N2 1.312(4), N1−C1 1.366(4), N1−B1−B2 123.8(3), B1−B2−P1 112.5(2), B2−P1−N2 106.45(14), P1−N2−C1 129.8(2), N2−C1−N1 125.0(3).

https://doi.org/10.1021/jacs.0c12627
J. Am. Chem. Soc. 2021, 143, 4993−5002

as indicated by the length of the C1−N1 and C1−N2 bonds. This results in lengthening of the N−B bond (N1−B1 1.526(4) Å) in comparison with that of **1**. The length of the B2−B1 bond (1.562(5) Å) falls in the range of B═B double-bond lengths (1.546−1.625 Å) in similar Lewis base-diborene complexes.[11−25] The NHC (B1−C20 1.590 Å) and phosphine (P1−B2 1.852(3) Å) of the phosphinoamidinate ligand are bonded with the B═B bond. Their bond lengths are similar to those of other NHC/phosphine-diborene complexes (C−B 1.532−1.603 Å, P−B 1.863−1.929 Å).[11−25]

DFT calculations (M06-2X/def2-TZVP, Figure S68) were performed to elucidate the electronic structure of **2**. The HOMO-1 shows the σ orbital of the B═B double bond arising from the mixing of B 2p orbitals (Figure 4). The HOMO

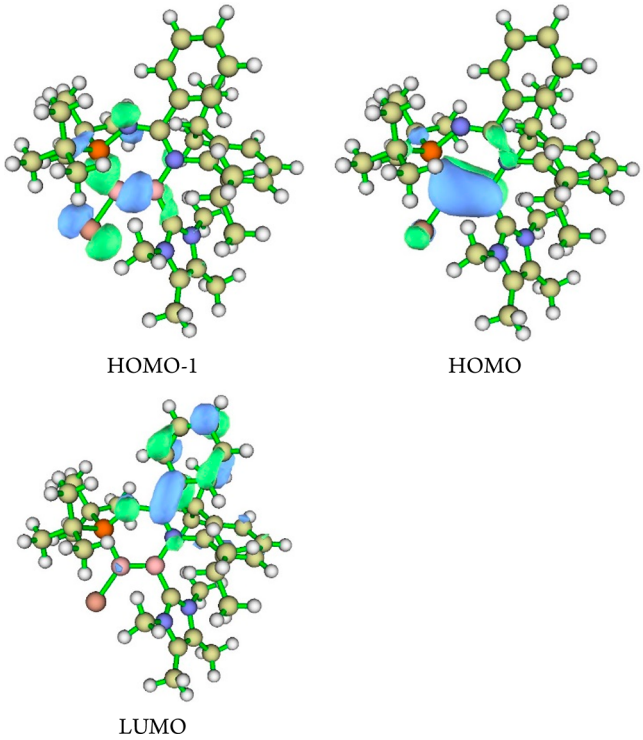

Figure 4. Calculated frontier orbitals of compound **2** (B, pink; Br, brown; C, yellow; H, white; N, blue; P, orange).

exhibits the π orbital of the B═B double-bond, while the LUMO represents the N 2p orbital conjugated with the π system of the phenyl group. Accordingly, a natural bond orbital (NBO, Table S8) analysis illustrates that the B1−B2 σ bond arises from the mixing of sp hybrids on the boron atoms (B1, $sp^{1.31}$; B2, $sp^{1.41}$). The B1−B2 π bond is slightly polarized toward the B1 atom (54.2% B1 + 45.8% B2). It is generated by the mixing of B p orbitals. The Wiberg bond index of 1.55 suggests that the B2−B1 bond is a double bond. In addition, natural population analysis (NPA) shows that the charges on the B1 and B2 atoms are −0.55 and 0.09 e, respectively. The dissected nucleus-independent chemical shift ($NICS_{zz}(1)$, −4.6 ppm; Table S9) shows that the diboron-containing six-membered ring in **2** is slightly aromatic.

The B═B double-bond character in **2** was illustrated by its reactivity with NH_3BH_3 in toluene at −78 °C (Scheme 2). The reaction mixture was warmed to room temperature and stirred for 3 h. The precipitate that formed in the reaction mixture was discarded by filtration. After that, the borylboronium cation **3**

Scheme 2. Synthesis of 3

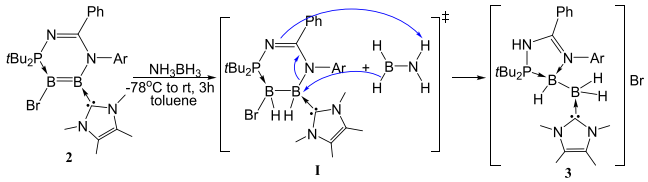

was isolated as a colorless crystalline solid from the concentrated filtrate. It is proposed that the reaction proceeds through the addition of H^+ and H^- from NH_3BH_3 to the B═B double bond in **2** to form the diborane intermediate **I** and NH_2BH_2. The second pair of H^+ and H^- from NH_2BH_2 attacks the *N*-phosphinoamidinate ligand and NHC-borane center, respectively, to form the *N*-phosphinoamidine ligand, which then displaces the Br^- moiety to form **3**. Its ^1H NMR spectrum exhibits signals for the *N*-phosphinoamidine and IMe backbone. The B−*H* signal cannot be found in the spectrum due to the quadrupolar boron nucleus. The $^{31}P\{^1H\}$ NMR spectrum shows a multiplet at 85.6 ppm due to the coupling with N−H and B−H protons. The $^{11}B\{^1H\}$ NMR spectrum shows two broad signals for the boronium cation (−14.2 ppm) and borane center (−36.2 ppm). The molecular structure of **3** obtained by X-ray crystallography (Figure 5) illustrates that the

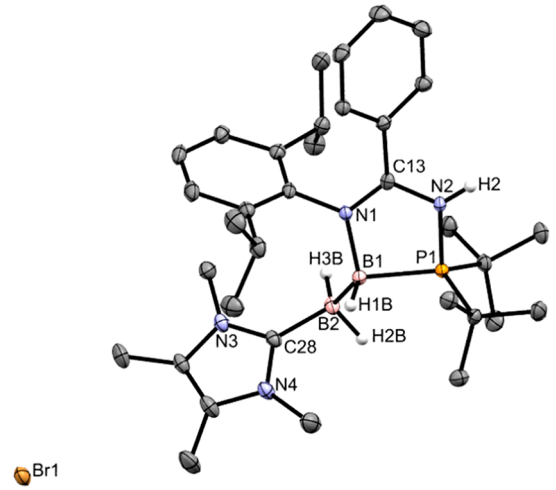

Figure 5. Molecular structure of **3** obtained by X-ray crystallography. Thermal ellipsoids are displayed at the 50% probability level. All H atoms are omitted for clarity. Selected bond lengths (Å) and angles (deg): B2−B1 1.749(4), C28−B2 1.603(3), N1−B1 1.617(3), P1−B1 1.970(2), P1−N2 1.6987(19), N2−C13 1.360(3), N1−C13 1.313(3), N1−B1−P1 96.19(14), N1−B1−B2 120.62(19), P1−B1−B2 116.79(16), B1−B2−C28 114.2(2).

N-phosphinoamidine chelates to the boronium B1 cation, while IMe coordinates to the borane B2 atom (C28−B2 1.603(3) Å). Both boron centers adopt a tetrahedral geometry. The B1···Br distance is 9.331 Å, indicating that there is no interaction between these atoms. The length of the B2−B1 bond is 1.749(4) Å. It is comparable to the B−B single-bond length in compound **1** (1.704(5) Å). The N1−B1 bond (1.617(3) Å) is considerably lengthened in comparison with the N−B single-bond length (1.428(5) Å) in compound **1**, indicating that the former is a coordinative covalent bond. In addition, the B1−P1 bond (1.970(2) Å) is comparable with the B−P coordinative covalent bond (1.940(4) Å) in

https://doi.org/10.1021/jacs.0c12627
J. Am. Chem. Soc. 2021, 143, 4993−5002

compound **1**. These data support that the *N*-phosphinoamidine ligand chelates the boronium B1 cation.

Compound **2** was capable of activating a small molecule, namely carbon dioxide (CO_2, 1 atm), in toluene at room temperature (Scheme 3). The reaction mixture changed from

Scheme 3. Formation of Compounds 4 and 5

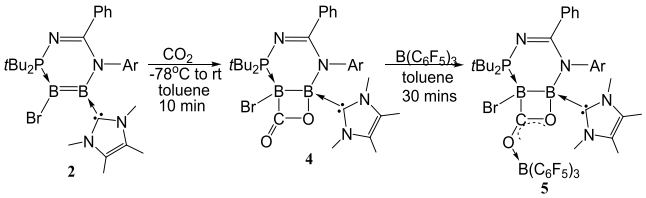

reddish purple to colorless immediately. After the reaction mixture was filtered, compound **4** was isolated as a colorless crystalline solid from the concentrated filtrate. In the reaction, the B═B double bond in **2** undergoes a [2 + 2] cycloaddition with CO_2 to give compound **4**. Its ^{1}H NMR spectrum displays signals of the *N*-phosphinoamidinate and IMe ligand. The $^{11}B\{^1H\}$ NMR signals are at −5.5 and −17.9 ppm, which are shifted upfield in comparison with those of compound **2**, demonstrating that the boron centers are four-coordinate. Moreover, the $^{31}P\{^1H\}$ NMR signal (39.7 ppm), which is comparable with that of compound **1**, is shifted upfield in comparison to that of compound **2**. These spectroscopic data indicate that the B−B bond in compound **4** is a single bond. This is consistent with the molecular structure of **4** (Figure 6)

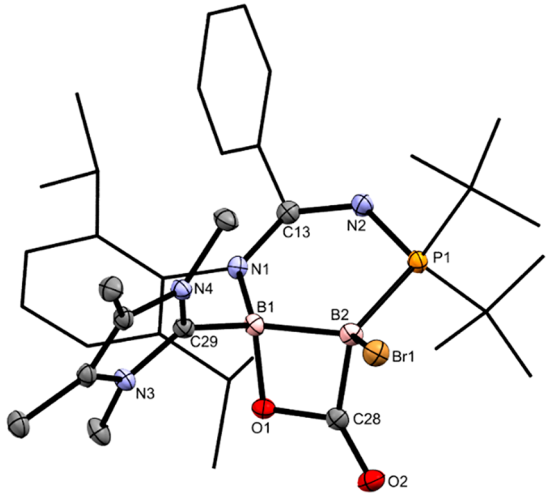

Figure 6. Molecular structure of **4** obtained by X-ray crystallography. Thermal ellipsoids are illustrated at the 50% probability level. All hydrogen atoms are omitted for clarity. Selected bond lengths (Å) and angles (deg): B2−B1 1.770(3), B2−C28 1.625(3), B1−O1 1.538(3), O1−C28 1.349(3), O2−C28 1.218(3), B2−P1 1.940(2), B1−N1 1.562(3), B1−C29 1.632(3), N1−B1−B2 118.67(17), B1−B2−P1 109.43(14), B1−B2−C28 78.73(15), B2−C28−O1 98.72(17), C28−O1−B1 96.48(15), O1−B1−B2 86.06(15).

obtained by X-ray crystallography, where the length of the B−B bond (1.770(3) Å) is comparable with that of the B−B single bond in compound **1**. The B_2CO four-membered ring is planar with the endocyclic O1−C28 bond (1.349(3) Å) being longer than the exocyclic O2−C28 bond (1.218(3) Å). In addition, the Br and IMe moieties are positioned in a *cis* fashion in reference to the boron-containing four-membered ring. Compound **4** is stable in solution and the solid state and does not decompose in refluxing toluene. Recently, Braunschweig et al. reported that the treatment of the NHC-diborene [IPr(Br)BB(Br)IPr] (IPr = :C{N(2,6-*i*Pr$_2$C$_6$H$_3$)CH}$_2$) with CO_2 formed a [2 + 2] cycloaddition product, which was thermally unstable and could not be isolated in quantity. It rearranged to form the 2,4-diboraoxetan-3-one containing oxo and carbonyl groups bridging between two boron centers.[26]

It is anticipated that the activated CO_2 moiety in compound **4** can be further functionalized. As such, compound **2** was treated with CO_2 and tris(pentafluorophenyl)borane in toluene at room temperature, where the reaction mixture instantly changed from red-purple to colorless (Scheme 3). After it was stirred for 30 min, the solution was filtered. Compound **5** was isolated as colorless crystals from the concentrated filtrate. The reaction proceeds through the formation of compound **4**, where the exocyclic C═O double bond further coordinates to $B(C_6F_5)_3$ to form compound **5**. Its $^{11}B\{^1H\}$ NMR signals (−5.7, −20.3 ppm) are comparable with those of **4**, indicating the presence of a B_2CO four-membered ring. Moreover, the $^{11}B\{^1H\}$ NMR signal of −26.9 ppm is attributable to the four-coordinate $B(C_6F_5)_3$. The molecular structure of **5** obtained by X-ray crystallography illustrates that the electronic structure of the B_2CO four-membered ring in **5** is different from that of **4** (Figure 7). The O1−C28 (1.292(4)

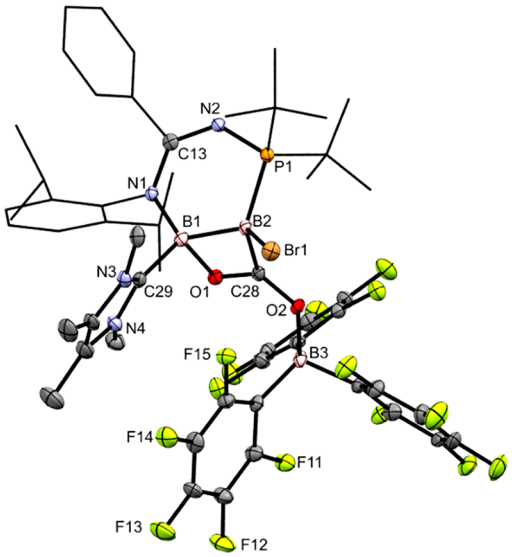

Figure 7. Molecular structure of **5** obtained by X-ray crystallography. Thermal ellipsoids are set at the 50% probability level. All hydrogen atoms are deleted for clarity. Selected bond lengths (Å) and angles (deg): B1−B2 1.791(6), B2−C28 1.593(5), B1−O1 1.625(5), O1−C28 1.292(4), O2−C28 1.280(4), O2−B3 1.551(5), B2−P1 1.950(4), B1−N1 1.544(5), C29−B1 1.619(6), N1−B1−B2 121.2(3), O1−B1−B2 83.8(2), B1−B2−P1 106.6(2), B1−B2−C28 77.6(2), B2−C28−O1 104.2(3), C28−O1−B1 92.9(3), O1−C28−O2 122.7(3), B2−C28−O2 132.5(3), C28−O2−B3 128.1(3).

Å) and O2−C28 (1.280(4) Å) bond lengths are almost identical, indicating that the double bond in the exocyclic C═O bond delocalizes along the O_{endo}−C−O_{exo} skeleton. The B2−C28 (1.593(5) Å) bond is shortened and the B1−O1 (1.625(5) Å) bond is lengthened in comparison with those in compound **4**. The experimental results show that **5** should be comprised of canonical forms, as illustrated in Scheme 4.

https://doi.org/10.1021/jacs.0c12627
J. Am. Chem. Soc. 2021, 143, 4993−5002

Scheme 4. Resonance Structures of 5

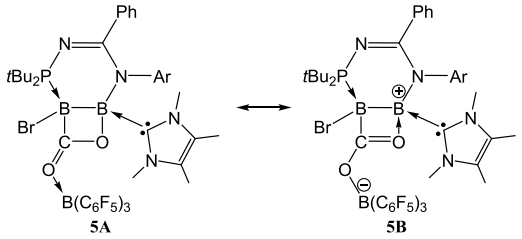

It is anticipated that, if $B(C_6F_5)_3$ in **5** is replaced by HBpin, the B−H bond could attack the C═O bond to form the formoxyborane [pinBOC(O)H] and regenerate compound **2**. As such, compound **2** should show catalytic reactivity toward CO_2. To begin with, no reaction between carbon dioxide (CO_2) and pinacolborane (HBpin) in deuterated benzene (C_6D_6) at 110 °C was observed. A 2 mol % portion of **2** was then used to catalyze the reaction of CO_2 with HBpin in C_6D_6 at room temperature (Table S1). In the first 1 h, a mixture of the formoxyborane [pinBOC(O)H] (**6a**, reaction time 1 h, yield 7.5%; Figure S21) and bis(boryl)oxide [$(pinB)_2O$] (**6c**, reaction time 1 h, yield 8.2%) were formed. After 20 h, the conversion was still less than 30% and only **6c** was observed (reaction time 20 h, yield 26%). When the reaction temperature was increased to 110 °C (Scheme 5), the catalytic reaction was much more efficient and extremely clean (conversion >99%), forming a mixture of the methoxyborane [pinBOMe] (**6b**, yield 97.8%, TOF 33.3 h^{-1}; Figure S22) and **6c** in a 1:1 ratio. The activity of compound **2** is outstanding when the turnover frequency and product yield are considered. The turnover frequency (TOF) far surpasses those of main-group-element hydride compounds (TOF (h^{-1}): Mg, 0.07; Ca, 0.1; Ge, 2.1; Sn, 14.5) for such catalysis.[27] Our results are different from thsoe for the NHC-dialumene-catalyzed hydroboration of CO_2 with HBpin, where 80% conversion of CO_2 to [pinBOC(O)H] was achieved at 80 °C for 3 h via the dialuminum carbonate active catalyst.[8]

Scheme 5. Catalytic Hydroboration of CO_2

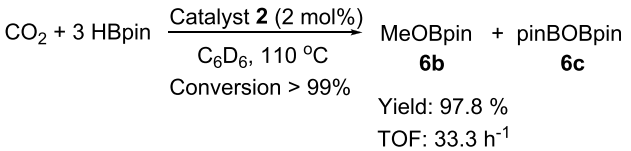

When the more sterically hindered 9-BBN (9-borabicyclo[3.3.1]nonane) was used instead of HBpin (Table S2 and Figure S25), 2 mol % of **2** catalyzed the hydroboration of CO_2 in C_6D_6 at 110 °C to form small amounts of formoxyborane **7a** at time zero. When the reaction continued to proceed, bis(boryl)acetal (**7b**, reaction time 1 h, yield 27.5%) and methoxyborane (**7c**, reaction time 20 h, yield 92%) were sequentially observed. The chronological formation of hydroborated products suggest that the B═B double bond was recurrently restored in a catalytic cycle. Therefore, the B═B double bond in compound **2** is the active site in the catalytic hydroboration of CO_2.

To prove that compound **4** is an intermediate in the catalysis, 2 mol % of **4** was utilized to mediate the catalytic reaction of CO_2 and HBpin in deuterated benzene (C_6D_6) at 110 °C for 2 h to afford a mixture of **6b** (yield 92.7%, TOF 23.6 h^{-1}) and **6c** in a 1:1 ratio. This illustrates that compound **4** further reacts with HBpin to form a zwitterionic moiety in resemblance of compound **5**.

On the basis of these experimental studies, the catalytic cycle for the hydroboration of CO_2 with HBpin is proposed

Scheme 6. DFT Calculations of the Catalytic Mechanism

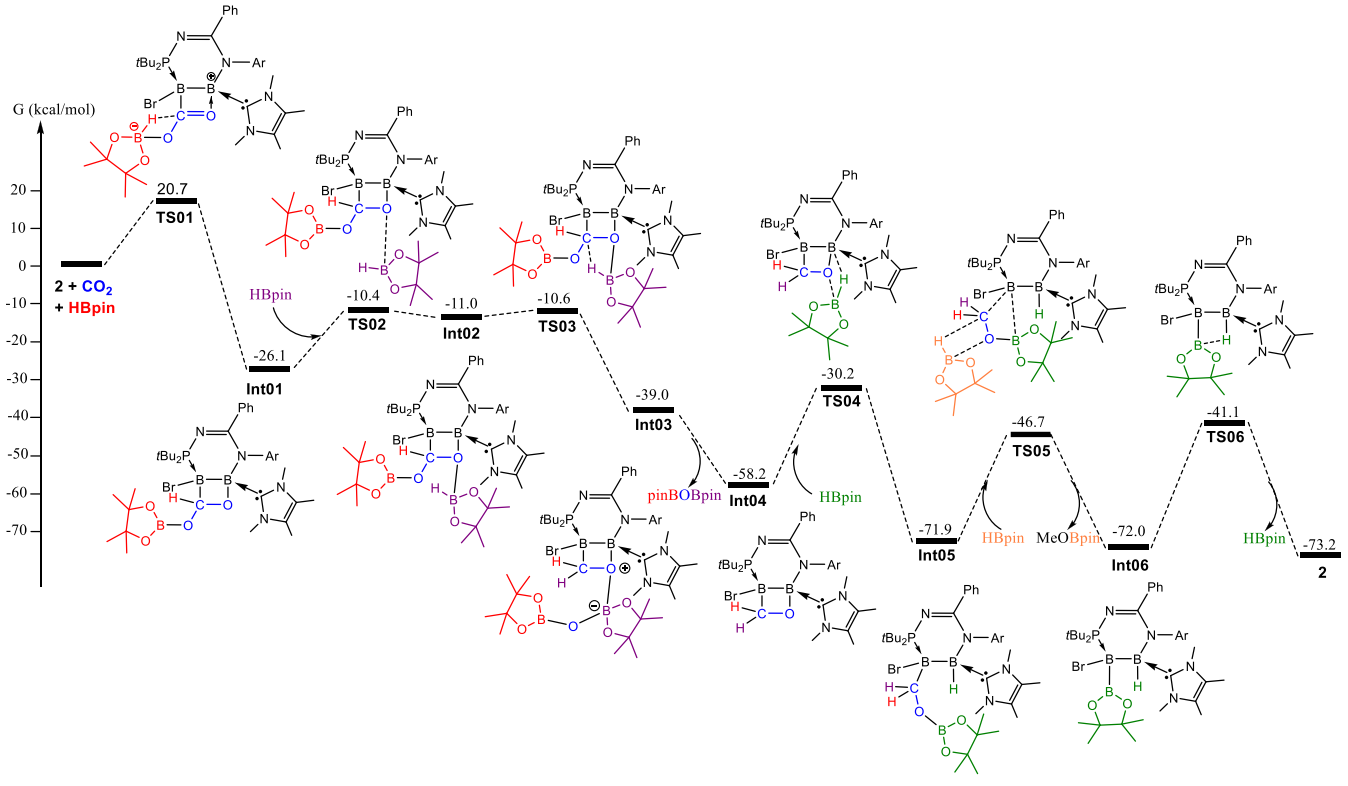

https://doi.org/10.1021/jacs.0c12627
J. Am. Chem. Soc. 2021, 143, 4993−5002

(Scheme 6) and has been studied by DFT calculations (M06-2X/def2-TZVP//M06-2X/def2-SVP/SMD(benzene)). The B═B double bond in **2** activates CO_2 with HBpin via **TS01** (ΔG = 20.7 kcal/mol). Subsequently, the H−B bond undergoes nucleophilic attack to the C═O bond to form **Int01** (ΔG = −26.1 kcal/mol). It appears as a [2 + 2] cycloaddition between **2** and the formoxyborane [HC(O)-OBpin]. The second HBpin then coordinates with the acetal oxygen atom in **Int01** via **TS02** (ΔG = −10.4 kcal/mol) to give **Int02** (ΔG = −11.0 kcal/mol). Its B−H bond attacks the acetal carbon atom via **TS03** (ΔG = −10.6 kcal/mol), which induces nucleophilic attack of OBpin, leading to the formation of pinBOBpin coordinated to the formaldehyde oxygen atom in **Int03** (ΔG = −39.0 kcal/mol). At this point, it is obvious that the first two C−H bond formations are kinetically facile processes. The steric effect between IMe and pinBOBpin leads to dissociation of the latter to form **Int04** (ΔG = −58.2 kcal/mol). **Int04** is considered as a [2 + 2] cycloaddition product between **2** and a formaldehyde. The B−O bond in **Int04** reacts with the B−H bond of the third HBpin. It proceeds through σ-bond metathesis at **TS04** ($\Delta G^{\ddagger}$ = −30.2 kcal/mol) to form **Int05** (ΔG = −71.9 kcal/mol). The fourth HBpin then reacts with **Int05**. The B−H bond attacks the methylene carbon at **TS05** ($\Delta G^{\ddagger}$ = −46.7 kcal/mol), which results in cleaving the $B-C_{methylene}$ bond and forming the B−Bpin bond. These lead to the formation of **Int06** and MeOBpin (ΔG = −72.0 kcal/mol). **Int06** undergoes 1,2-elimination of HBpin via **TS06** ($\Delta G^{\ddagger}$ = −41.1 kcal/mol) to generate **2** and HBpin (ΔG = −73.2 kcal/mol). The computed barriers of **Int04→TS04** (28.0 kcal/mol) and **Int06→TS06** (30.9 kcal/mol) are consistent with the catalysis requiring 110 °C to occur. The calculated results are in accordance with the experimental conditions and observations. A reaction temperature of 25 °C resulted in **6c** with 26% yield (20 h), suggesting that the reaction ends at **Int04**. A reaction temperature of 110 °C provides sufficient energy to overcome the kinetic barrier (**TS04** and **TS06**), and hence a mixture of **6b** and **6c** was formed in a 1:1 ratio.

Then, the catalytic ability of **2** toward N-formylation of primary and secondary amines by carbon dioxide and pinacolborane was examined (Table 1 and Table S3). To begin with, compound **2** (5 mol %) cannot catalyze the reaction of **8e** and carbon dioxide (CO_2) at 90 °C without pinacolborane (HBpin, Table S4). However, 5 mol % of **2** catalyzed the N-formylation of the primary aliphatic *n*-butylamine **8b** and 3-methoxypropan-1-amine **8c** with CO_2 and HBpin in deuterated benzene (C_6D_6) at 90 °C to yield the corresponding N-formamides (yield (%) (TOF (h^{-1})): **9b**, 95 (40.0); **9c**, 96 (40.0)), bis(boryl)oxide **6c**, and H_2. Second, a high yield and TOF were accomplished for the N-formylation of aliphatic secondary diethylamine **8d** (yield 92%, TOF 50 h^{-1}), diisopropylamine **8a** (yield 98%, TOF 13.3 h^{-1}), and piperidine **8e** (yield 98%, TOF 33.3 h^{-1}). Third, aromatic *N*-methylaniline **8f** (yield 81%, TOF 3.1 h^{-1}) and indoline **8g** (yield 91%, TOF 1.4 h^{-1}) were less active in the catalyses. It is noteworthy that compound **2** is one of the rare main-group catalysts that mediate N-formylation using carbon dioxide and pinacolborane, including the NHC-silyliumylidene cation $[(IMe)_2SiH]I$.[28] Moreover, **2** exceeds the latter in view of both reaction time and TOF (example of $[(IMe)_2SiH]I$, **9a**: yield 68%, TOF 6.8 h^{-1}). Other main-group-element catalysts, namely proazaphosphatrane[29] and carbodicarbene,[30] can only use the potent 9-BBN for the N-methylation of amines with carbon dioxide. To understand the catalytic mechanism, piperidine **8e** was reacted with HBpin in C_6D_6 at 90 °C, resulting in the formation of the borylamine and H_2. This suggests that the formation of H_2 in the above catalysis arose from the coupling reaction of amines and HBpin. In this context, a catalytic mechanism is proposed (Scheme 7).

Table 1. 2-Catalyzed N-formylation[a]

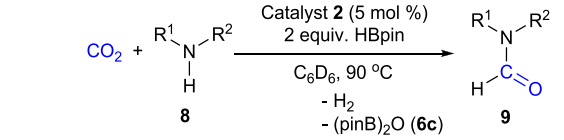

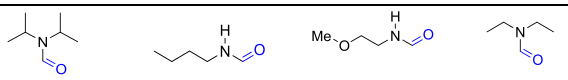

9a	9b	9c	9d
>99 (98)%, 13.3 h^{-1}	>99 (95)%, 40.0 h^{-1}	>99 (96)%, 40.0 h^{-1}	>99 (92)%, 50 h^{-1}

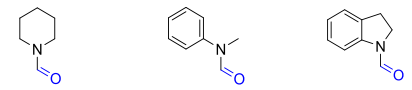

9e	9f	9g
>99 (98)%, 33.3 h^{-1}	91 (81)%, 3.1 h^{-1}	82 (81)%, 1.4 h^{-1}

[a]Reaction conditions: Amine (0.10 mmol), HBpin (0.20 mmol, 2 equiv), **2**a (5 mol %), C_6D_6 (0.50 mL), and CO_2 (1 bar). Yields were calculated by ^1H NMR spectroscopy on the basis of the amount of the consumed amine with reference to cyclohexane (internal standard). They are reported in parentheses. $R^1R^2NC(O)H$ was identified as the sole product. All reactions were performed three times.

Scheme 7. Proposed Catalytic N-formylation Mechanism

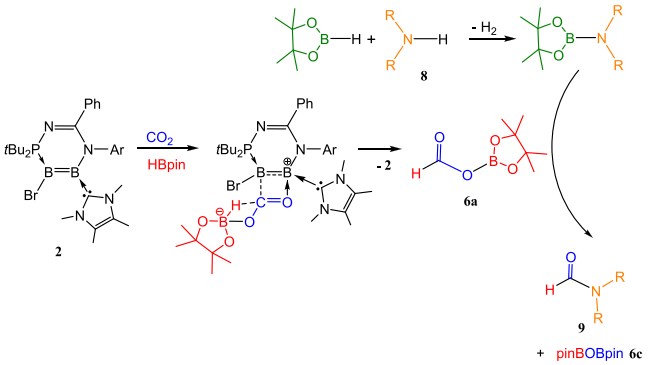

Compound **2** catalyzes the reaction of CO_2 and HBpin to form formoxyborane [pinBOC(O)H] (**6a**). This then undergoes a substitution reaction with borylamine, which is formed by the dehydrogenation reaction of amine and HBpin, to form N-formamide and pinBOBpin **6c**.

In addition to the catalytic hydroboration of carbon dioxide and N-formylation, **2** (5 mol %) was able to catalyze the chemoselective hydroboration of aldehyde and ketone **10** in C_6D_6 at room temperature to form borate esters (**11**, 16 examples: aldehydes, yield = 99%, TOF = 4−120 h^{-1}; ketones, yield = 80−98%, TOF = 0.4−10 h^{-1}; Scheme 8 and Table S5). The results further support that compound **2** is an active catalyst in >C═O hydroboration.

https://doi.org/10.1021/jacs.0c12627
J. Am. Chem. Soc. 2021, 143, 4993−5002

Scheme 8. Chemoselective Hydroboration of Carbonyl Compounds

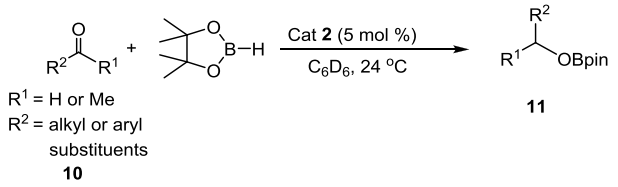

CONCLUSION

In conclusion, the phosphinoamidinato NHC-diborene compound **2** is a multiply bonded boron catalyst showing catalytic capability toward the hydroboration of CO_2 with HBpin and N-formylation of primary and secondary amines by CO_2 and HBpin, as well as chemoselective hydroboration of carbonyl compounds. In particular, compound **2** efficiently reduces CO_2 with HBpin to form MeOBpin and pinBOBpin. Its catalytic activity is superior to that of existing main-group-element catalysts employed for such reactions. In the mechanistic studies, compound **2** exhibits reactivity resembling that of a transition metal in the catalytic hydroboration of CO_2. Its B═B double bond activated CO_2 with HBpin, the initial intermediate of which was further reacted with two HBpin molecules to form MeOBpin and pinBOBpin, along with the regeneration of **2**. It is anticipated that compound **2** can mediate a variety of other catalytic reactions, and they are currently under investigation.

EXPERIMENTAL SECTION

General Procedure. All experiments were performed under an argon gas atmosphere by standard Schlenk procedures. Chemicals were acquired from Sigma-Aldrich and utilized directly without further purification. All solvents were dried over K metal or CaH_2 prior to use. ^1H, $^{11}B\{^1H\}$, $^{13}C\{^1H\}$, and $^{31}P\{^1H\}$ NMR spectroscopy were performed using a JEOL ECA 400 MHz spectrometer. All NMR spectra were recorded in deuterated benzene. The chemical shifts (ppm) are respective to $SiMe_4$ for ^{13}C and ^1H, $BF_3{\cdot}Et_2O$ for ^{11}B, and 85% H_3PO_4 for ^{31}P, respectively. HRMS spectrometry was carried out at the Division of Chemistry and Biological Chemistry (Mass Spectrometry Laboratory), Nanyang Technological University. Melting points were recorded using an OptiMelt automated melting point instrument.

Synthesis of 1. A solution of *n*BuLi (2.6 M, 0.4 mL, 1.05 mmol) in hexane was placed in a 100 mL Schlenk flask containing a stirred diethyl ether solution of *N*-phosphinoamidine (0.425 g, 1 mmol) at −78 °C, following which, the solution was warmed to room temperature and stirred for 3 h. The resulting yellow solution was dried under vacuum to remove all volatiles. A solution of $B_2Br_4(SMe_2)_2$(0.466 g, 1 mmol) in toluene was then slowly placed in the Schlenk flask at −78 °C. The reaction mixture was stirred at room temperature for 12 h and then was filtered. The filtrate was then concentrated and stored at 4 °C for 2 days to give **1** as a colorless crystalline solid (0.52 g, 76% yield). Mp: 177 °C. ^1H NMR (399.5 MHz, 25 °C, C_6D_6): δ 7.33−7.30 (m, 2 H, Ar*H*), 7.05−6.77 (m, 6 H, Ar*H*), 3.38 (sept, 2 H, C*H*Me$_2$, J_{HH} = 6.8 Hz), 1.44 (d, 18 H, *tBu*, J_{PH} = 14.2 Hz), 1.32 (d, 6 H, CH*Me*$_2$, J_{HH} = 6.8 Hz), 0.93 (d, 6 H, CH*Me*$_2$, J_{HH} = 6.8 Hz). $^{11}B\{^1H\}$ NMR (128 MHz, 25 °C, C_6D_6): δ 55.50 (s), −11.94 (s). $^{31}P\{^1H\}$ NMR (162 MHz, 25 °C, C_6D_6): δ 35.72 (br). $^{13}C\{^1H\}$ NMR (101 MHz, 25 °C, C_6D_6): 168.14 (d, J = 11.6 Hz, N*C*N), 145.41 (*C*H-Ar), 140.05 (*C*H-Ar), 138.74 (d, J = 13.5 Hz, *C*-Ar), 129.44 (*C*H-Ar), 128.89 (*C*H-Ar), 128.78 (*C*H-Ar), 128.45 (*C*H-Ar), 127.62 (*C*H-Ar), 126.99 (*C*-Ar), 124.45 (*C*-Ar), 38.28 (d, J = 34.8 Hz, P*C*(CH$_3$)), 28.62 (CH(*C*H$_3$)$_2$), 27.77 (PC(*C*H$_3$)), 25.14 (CH(*C*H$_3$)$_2$), 23.34 (CH(*C*H$_3$)$_2$). HRMS(ESI): m/z calcd for $C_{27}H_{41}B_2{}^{79}Br_3N_2P$, 683.0744 [$(M + H)$]$^+$; found, 683.0761.

Synthesis of 2. A toluene solution of 1,3,4,5-tetramethylimidazolin-2-ylidene (IMe, 0.149 g, 1.2 mmol) was placed in a 100 mL Schlenk flask containing **1** (0.685 g, 1 mmol) at room temperature. After 10 min, the reaction mixture turned red with some precipitate. The resulting suspension was stirred for 4 h. Subsequently, it was filtered and the pale red residue was then dried under vacuum for 2 h. The red residue was the adduct **1**·IMe adduct and was used without further purification. A 30 mL portion of toluene was placed in a 100 mL Schlenk flask containing a mixture of **1**·IMe (0.809 g, 1 mmol) and excess potassium graphite (0.54 g, 4 mmol) at room temperature, causing the reaction mixture to turn purplish red immediately. The resulting suspension was stirred for 3 h and filtered. The filtrate was concentrated to 5 mL and stored at −20 °C for 1 day to give **2** as a red crystalline solid (0.24 g, 37% yield). Mp: 198 °C dec. ^1H NMR (399.5 MHz, 25 °C, C_6D_6): δ 7.66−7.64 (m, 2 H, Ar*H*), 7.05−6.88 (m, 6 H, Ar*H*), 3.37 (sept, 2 H, C*H*Me$_2$, J_{HH} = 7.2 Hz), 3.19 (s, 6 H, N-C*H*$_3$), 1.71 (d, 18 H, *tBu*, J_{PH} = 12.8 Hz), 1.23 (s, 6 H, C-C*H*$_3$), 0.85 (d, 6 H, CH*Me*$_2$, J_{HH} = 6.4 Hz), 0.80 (d, 6 H, CH*Me*$_2$, J_{HH} = 6.8 Hz). $^{11}B\{^1H\}$ NMR (128 MHz, 25 °C, C_6D_6): δ 30.64, 9.16. $^{31}P\{^1H\}$ NMR (162 MHz, 25 °C, C_6D_6): δ 45.93 (br). $^{13}C\{^1H\}$ NMR (101 MHz, 25 °C, C_6D_6): 152.85 (*C*-carbene), 145.37 (*C*H-Ar), 144.46 (*C*H-Ar), 141.05 (d, J = 16.4 Hz, *C*-Ar), 130.72 (*C*H-Ar), 129.01 (*C*H-Ar), 128.25 (*C*H-Ar), 127.62 (*C*H-Ar), 126.90 (*C*H-Ar), 126.70 (*C*-Ar), 126.65 (*C*-Ar), 124.13 (*C*-Ar), 123.04 (*C*CH$_3$), 38.65 (d, J = 42.5 Hz, P*C*(CH$_3$)), 33.13 (N*C*H$_3$), 28.47 (*C*H(CH$_3$)$_2$), 27.72 (d, J = 1.9 Hz, PC(*C*H$_3$)), 24.95 (CH(*C*H$_3$)$_2$), 23.55 (CH(*C*H$_3$)$_2$), 7.82 (*C*H$_3$). HRMS(ESI): m/z calcd for $C_{34}H_{53}B_2{}^{79}BrN_4P$, 649.3377 [$(M + H)$]$^+$; found, 649.3395.

Synthesis of 3. A 20 mL portion of toluene was placed in a 100 mL Schlenk flask containing **2** (0.130 g, 0.2 mmol) and NH_3BH_3 (0.007 g, 0.2 mmol) at −78 °C. The resulting solution was warmed to room temperature and stirred for 3 h with the color changing from red-purple to pale red. The reaction solution was filtered. The filtrate was then concentrated and kept at room temperature to give **3** as a colorless crystalline solid (0.07 g, 54% yield). Mp: 147 °C. ^1H NMR (399.5 MHz, 25 °C, C_6D_6): δ 7.78−7.76 (m, 2 H, Ar*H*), 6.87−7.04 (m, 4 H, Ar*H*), 6.75−6.69 (m, 2 H, Ar*H*), 3.29 (sept, 1 H, C*H*Me$_2$, J_{HH} = 7.2 Hz), 2.78 (sept, 1 H, C*H*Me$_2$, J_{HH} = 7.2 Hz), 2.61 (s, 6 H, N-C*H*$_3$), 1.78 (dd, 18 H, *tBu*, J_{PH} = 14.2 Hz, J_{PH} = 15.1 Hz), 1.44 (d, 3 H, CH*Me*$_2$, J_{HH} = 6.4 Hz), 1.27 (s, 6 H, C-C*H*$_3$), 1.11 (d, 3 H, CH*Me*$_2$, J_{HH} = 6.8 Hz), 0.46 (d, 3 H, CH*Me*$_2$, J_{HH} = 6.8 Hz), 0.12 (d, 3 H, CH*Me*$_2$, J_{HH} = 6.8 Hz). $^{11}B\{^1H\}$ NMR (128 MHz, 25 °C, C_6D_6): δ −14.24 (br), −34.15 (br). $^{31}P\{^1H\}$ NMR (162 MHz, 25 °C, C_6D_6): δ 85.62 (br). $^{13}C\{^1H\}$ NMR (101 MHz, 25 °C, C_6D_6): 167.13 (d, J = 11.5 Hz, N*C*N), 145.90 (*C*-carbene), 144.89 (*C*H-Ar), 143.81 (*C*H-Ar), 139.24 (d, J = 8.6 Hz, *C*-Ar), 132.17 (*C*H-Ar), 131.83 (*C*H-Ar), 130.23 (*C*H-Ar), 126.70 (*C*H-Ar), 126.11 (*C*H-Ar), 125.25 (*C*-Ar), 124.63 (*C*-Ar), 124.38 (*C*-Ar), 123.74 (*C*CH$_3$), 121.75 (*C*CH$_3$), 37.72 (d, J = 23.1 Hz, P*C*(CH$_3$)), 35.50 (d, J = 25.1 Hz, P*C*(CH$_3$)), 34.68 (N*C*H$_3$), 31.50 (N*C*H$_3$), 28.64 (*C*H(CH$_3$)$_2$), 28.08 (d, J = 28.9 Hz, PC(*C*H$_3$)), 27.74 (d, J = 28.9 Hz, PC(*C*H$_3$)), 25.48 (*C*H(CH$_3$)$_2$), 24.80 (CH(*C*H$_3$)$_2$), 23.94 (CH(*C*H$_3$)$_2$), 23.10 (CH(*C*H$_3$)$_2$), 22.67 (CH(*C*H$_3$)$_2$), 7.89 (*C*H$_3$), 7.58 (*C*H$_3$). HRMS (ESI): m/z calcd for $C_{34}H_{57}B_2{}^{79}BrN_4P$, 653.3690 [$(M + H)$]$^+$; found, 653.3705.

Synthesis of 4. A toluene solution of **2** (0.130 g, 0.2 mmol) in a Schlenk flask was degassed by a freeze−pump−thaw method. Then, CO_2 (1 bar) was filled. The resulting solution changed from reddish purple to colorless immediately. After 10 min of stirring, the solution was filtered. The filtrate was concentrated and kept at −20 °C for 1 day to give **4** as a colorless crystalline solid (0.12 g, 88% yield). Mp: 193 °C. ^1H NMR (399.5 MHz, 25 °C, C_6D_6): δ 7.66−7.64 (m, 2 H, Ar*H*), 7.14−7.02 (m, 2 H, Ar*H*), 6.92−6.88 (m, 3 H, Ar*H*), 6.79−6.75 (m, 1 H, Ar*H*), 3.83 (sept, 1 H, C*H*Me$_2$, J_{HH} = 7.2 Hz), 3.63 (s, 3 H, N−C*H*$_3$), 2.83 (sept, 1 H, C*H*Me$_2$, J_{HH} = 7.2 Hz), 2.61 (s, 3 H, N-C*H*$_3$), 1.69 (d, 3 H, CH*Me*$_2$, J_{HH} = 7.3 Hz), 1.67 (dd, 18 H, *tBu*, J_{PH} = 7.3 Hz, J_{PH} = 8.2 Hz), 1.37 (s, 3 H, C-C*H*$_3$), 0.92 (d, 3 H, CH*Me*$_2$, J_{HH} = 6.8 Hz), 0.87 (s, 3 H, C-C*H*$_3$), 0.74 (d, 3 H, CH*Me*$_2$, J_{HH} = 6.4

https://doi.org/10.1021/jacs.0c12627
J. Am. Chem. Soc. 2021, 143, 4993−5002

Hz), 0.09 (d, 3 H, CH*Me*$_2$, J_{HH} = 6.8 Hz). $^{11}B\{^1H\}$ NMR (128 MHz, 25 °C, C_6D_6): δ −5.47, −17.86. $^{31}P\{^1H\}$ NMR (162 MHz, 25 °C, C_6D_6): δ 39.66 (br). $^{13}C\{^1H\}$ NMR (101 MHz, 25 °C, C_6D_6): 168.72 (d, J = 8.7 Hz, NCN), 148.99 (*C*-carbene), 144.31 (*C*H-Ar), 142.42 (*C*H-Ar), 141.10 (d, J = 15.4 Hz, *C*-Ar), 130.53 (*C*H-Ar), 128.52 (*C*H-Ar), 127.28 (*C*H-Ar), 127.10 (*C*H-Ar), 126.76 (*C*H-Ar), 125.71 (*C*-Ar), 124.72 (*C*-Ar), 124.45 (*C*-Ar), 123.88 (*C*CH$_3$), 123.72 (*C*CH$_3$), 38.46 (d, J = 44.3 Hz, P*C*(CH$_3$)), 38.08 (d, J = 44.3 Hz, P*C*(CH$_3$)), 34.37 (NCH$_3$), 31.85 (NCH$_3$), 28.64 (*C*H(CH$_3$)$_2$), 27.88 (d, J = 28.9 Hz, PC(*C*H$_3$)), 26.71 (*C*H(CH$_3$)$_2$), 25.66 (CH(*C*H$_3$)$_2$), 25.09 (CH(*C*H$_3$)$_2$), 24.86 (CH(*C*H$_3$)$_2$), 22.87 (CH(*C*H$_3$)$_2$), 7.53 (*C*H$_3$), 7.31 (*C*H$_3$). HRMS(ESI): m/z calcd for $C_{35}H_{53}B_2{}^{79}BrN_4O_2P$, 693.3276 $[(M + H)]^+$; found, 693.3302.

Synthesis of 5. A toluene solution of **2** (0.130 g, 0.2 mmol) and tris(pentafluorophenyl)borane (0.110 g, 0.2 mmol) in a Schlenk flask was degassed by a freeze−pump−thaw method. Subsequently, CO_2 (1 bar) was filled. The resulting solution changed from red-purple to colorless immediately. After 30 min of stirring, the solution was filtered. The filtrate was concentrated and kept at −20 °C for 1 day to afford **5** as a colorless crystalline solid (0.20 g, 84% yield). Mp: 161 °C. ^1H NMR (399.5 MHz, 25 °C, C_6D_6): δ 7.27−7.25 (m, 2 H, Ar*H*), 7.08−6.90 (m, 2 H, Ar*H*), 6.80−6.78 (m, 3 H, Ar*H*), 6.64−6.61 (m, 1 H, Ar*H*), 3.56 (s, 3 H, N-C*H*$_3$), 2.82 (sept, 1 H, C*H*Me$_2$, J_{HH} = 7.2 Hz), 2.49 (sept, 1 H, C*H*Me$_2$, J_{HH} = 7.2 Hz), 2.14 (s, 3 H, N-C*H*$_3$), 1.42 (dd, 18 H, *tBu*, J_{PH} = 13.7 Hz, J_{PH} = 15.1 Hz), 1.42 (s, 3 H, C-C*H*$_3$), 1.13 (s, 3 H, C-C*H*$_3$), 0.95 (d, 3 H, CH*Me*$_2$, J_{HH} = 6.4 Hz), 0.81 (d, 3 H, CH*Me*$_2$, J_{HH} = 6.8 Hz), 0.21 (d, 3 H, CH*Me*$_2$, J_{HH} = 6.8 Hz), 0.10 (d, 3 H, CH*Me*$_2$, J_{HH} = 6.8 Hz). $^{11}B\{^1H\}$ NMR (128 MHz, 25 °C, C_6D_6): δ −5.71, −20.32, −26.89. $^{19}F\{^1H\}$ NMR (376 MHz, 25 °C, C_6D_6): δ −131.31 (s, 1 F), −159.34 (t, 1 F, J = 21.7 Hz), −164.69 (dt, 1 F, J = 21.7, 21.7 Hz). $^{31}P\{^1H\}$ NMR (162 MHz, 25 °C, C_6D_6): δ 37.44 (br). $^{13}C\{^1H\}$ NMR (101 MHz, 25 °C, C_6D_6): δ 168.48 (d, J = 8.7 Hz, NCN), 149.56 (*C*-F), 147.42 (*C*-carbene), 147.11 (*C*-F), 144.05 (*C*H-Ar), 141.74 (*C*H-Ar), 139.66 (d, J = 16.3 Hz, *C*-Ar), 138.33 (*C*-F), 137.58 (*C*-F), 135.73 (*C*-F), 130.89 (*C*H-Ar), 129.27 (*C*H-Ar), 129.01 (*C*H-Ar), 128.24 (*C*H-Ar), 127.61 (*C*H-Ar), 126.81 (*C*-Ar), 126.16 (*C*-Ar), 125.95 (*C*-Ar), 125.72 (*C*-Ar), 125.37 (*C*CH$_3$), 123.58 (*C*CH$_3$), 39.34 (d, J = 45.7 Hz, P*C*(CH$_3$)), 37.94 (d, J = 39.5 Hz, P*C*(CH$_3$)), 35.79 (NCH$_3$), 32.10 (NCH$_3$), 28.31 (d, J = 38.5 Hz, PC(*C*H$_3$)), 27.54 (*C*H(CH$_3$)$_2$), 26.82 (CH(*C*H$_3$)$_2$), 25.03 (CH(*C*H$_3$)$_2$), 24.21 (CH(*C*H$_3$)$_2$), 22.20 (CH(*C*H$_3$)$_2$), 21.11 (CH(*C*H$_3$)$_2$), 7.60 (*C*H$_3$), 7.53 (*C*H$_3$). HRMS(ESI): m/z calcd for $C_{53}H_{53}B_3{}^{79}BrF_{15}N_4O_2P$, 1205.3129 $[(M + H)]^+$; found, 1205.3145.

Synthesis of Compounds 6a−c. Catalyst **2** (0.026 g, 0.04 mmol), cyclohexane (internal standard, 0.168 g, 2 mmol, 50 equiv), and deuterated benzene (0.5 mL) were placed in a J. Young NMR tube. HBpin (0.256 g, 2 mmol, 50 equiv) was subsequently added. After that, the J. Young NMR tube was dipped in liquified nitrogen, which froze the reaction mixture. It was degassed using a freeze−pump−thaw method. Carbon dioxide (1 bar) was then filled. The reaction mixture was warmed from room temperature to 110 °C for 1.5 h. The catalysis was monitored using ^1H NMR spectroscopy. The yields were calculated on the basis of the integration of ^1H NMR signals of pinBOMe (**6b**) at 1.05 and 3.51 ppm and (pinB)$_2$O (**6c**) at 1.02 ppm relative to the −C*H*$_2$ signal of cyclohexane (internal standard) at 1.37 ppm. The chemical shifts of the products agree with the reported values in the literature and independent *in situ* NMR-scale syntheses.[31]

Synthesis of Compounds 7a−d. Catalyst **2** (1.3 mg, 0.002 mmol), 9-BBN (0.012 g, 0.1 mmol, 50 equiv), and C_6D_6 (0.5 mL) were placed in a J. Young NMR tube. The solution was degassed by a freeze−pump−thaw method as described in the synthesis of **6a−c**. Carbon dioxide (1 bar) was then filled. After that, the resulting mixture was warmed from room temperature to 110 °C. The catalysis was checked by ^1H NMR spectroscopy at time intervals of 20 min, 40 min, 1 h, 4 h, 12 h, and 20 h. The NMR data are given in the Supporting Information.

Catalytic N-formylation of Secondary and Primary Amines by CO_2 and HBpin: General Procedure. In a J. Young NMR tube were placed catalyst **2** (0.0032 g, 0.005 mmol), cyclohexane (internal standard, 8.4 mg, 0.10 mmol), HBpin (0.0256 g, 0.20 mmol), amine (0.10 mmol) and deuterated benzene (0.5 mL). Subsequently, it was dipped in liquid nitrogen and the reaction mixture was frozen. It was degassed using s freeze−pump−thaw method. Carbon dioxide (1 bar) was subsequently filled. The details of the catalytic settings are given in Tables S3 and S4 in the Supporting Information. The catalysis was checked by ^1H NMR spectroscopy. The yields of products were calculated on the basis of the integration of ^1H NMR signals of $R^1R^2NC(=O)H$ at ca. 8 ppm relative to that of cyclohexane (C*H*$_2$, 1.37 ppm). The NMR data are given in the Supporting Information.

Catalytic Reaction of Aldehydes and Ketones with HBpin: General Procedure. Catalyst **2** (0.013 g, 0.02 mmol) and C_6D_6 (0.5 mL) were mixed in a J. Young NMR tube. Pinacolborane (0.052 g, 0.41 mmol, 20.1 equiv) and carbonyl compounds (0.40 mmol, 20 equiv) were subsequently added. The catalytic settings are given in Table S5. The catalyses were checked by ^1H NMR spectroscopy to calculate their yields. The chemical shifts of the products are consistent with the reported values in the literature.[31] All of the catalytic trials were performed three times.

■ ASSOCIATED CONTENT

Supporting Information

The Supporting Information is available free of charge at https://pubs.acs.org/doi/10.1021/jacs.0c12627.

Experimental procedures and DFT calculations (PDF)

Accession Codes

CCDC 2047677−2047681 contain the supplementary crystallographic data for this paper. These data can be obtained free of charge via www.ccdc.cam.ac.uk/data_request/cif, or by emailing data_request@ccdc.cam.ac.uk, or by contacting The Cambridge Crystallographic Data Centre, 12 Union Road, Cambridge CB2 1EZ, UK; fax: +44 1223 336033.

■ AUTHOR INFORMATION

Corresponding Authors

Ming-Der Su − *Department of Applied Chemistry, National Chiayi University, Chiayi 60004, Taiwan; Department of Medicinal and Applied Chemistry, Kaohsiung Medical University, Kaohsiung 80708, Taiwan;* orcid.org/0000-0002-5847-4271; Email: midesu@mail.ncyu.edu.tw

Cheuk-Wai So − *Division of Chemistry and Biological Chemistry, School of Physical and Mathematical Sciences, Nanyang Technological University, Singapore 637371;* orcid.org/0000-0003-4816-9801; Email: CWSo@ntu.edu.sg

Authors

Jun Fan − *Division of Chemistry and Biological Chemistry, School of Physical and Mathematical Sciences, Nanyang Technological University, Singapore 637371*

Jian-Qiang Mah − *Division of Chemistry and Biological Chemistry, School of Physical and Mathematical Sciences, Nanyang Technological University, Singapore 637371*

Ming-Chung Yang − *Department of Applied Chemistry, National Chiayi University, Chiayi 60004, Taiwan*

Complete contact information is available at: https://pubs.acs.org/10.1021/jacs.0c12627

Author Contributions

The manuscript was written through contributions of all authors.

Notes

The authors declare no competing financial interest.

■ ACKNOWLEDGMENTS

C.-W.S. thanks the Ministry of Education Singapore, AcRF Tier 2 (MOE2019-T2-2-129), and the National Research Foundation Singapore, NRF-ANR (NRF2018-NRF-ANR026 Si-POP), for the financial support. M.-C.Y. and M.-D.S. acknowledge the National Center for High-Performance Computing of Taiwan for generous amounts of computing time and the Ministry of Science and Technology of Taiwan for financial support.

■ REFERENCES

(1) (a) Power, P. P. Main-group Elements as Transition Metals. *Nature* **2010**, *463*, 171−177. (b) Braunschweig, H.; Dewhurst, R. D. Single, Double, Triple Bonds and Chains: The Formation of Electron-Precise B-B Bonds. *Angew. Chem., Int. Ed.* **2013**, *52*, 3574−3583. (c) Arrowsmith, M.; Braunschweig, H.; Stennett, T. E. Formation and Reactivity of Electron-Precise B-B Single and Multiple Bonds. *Angew. Chem., Int. Ed.* **2017**, *56*, 96−115. (d) Weetman, C.; Inoue, S. The Road Travelled: After Main-Group Elements as Transition Metals. *ChemCatChem* **2018**, *10*, 4213−4228. (e) Chu, T.; Nikonov, G. I. Oxidative Addition and Reductive Elimination at Main-Group Element Centers. *Chem. Rev.* **2018**, *118*, 3608−3680. (f) Légaré, M.-A.; Pranckevicius, C.; Braunschweig, H. Metallomimetic Chemistry of Boron. *Chem. Rev.* **2019**, *119*, 8231−8261.

(2) (a) Bag, P.; Porzelt, A.; Altmann, P. J.; Inoue, S. A Stable Neutral Compound with an Aluminum-Aluminum Double Bond. *J. Am. Chem. Soc.* **2017**, *139*, 14384−14387. (b) Weetman, C.; Porzelt, A.; Bag, P.; Hanusch, F.; Inoue, S. Dialumenes - Aryl vs. Silyl Stabilisation for Small Molecule Activation and Catalysis. *Chem. Sci.* **2020**, *11*, 4817−4827.

(3) (a) Braunschweig, H.; Dellermann, T.; Dewhurst, R. D.; Ewing, W. C.; Hammond, K.; Jimenez-Halla, J. O. C.; Kramer, T.; Krummenacher, I.; Mies, J.; Phukan, A. K.; Vargas, A. Metal-Free Binding and Coupling of Carbon Monoxide at a Boron-Boron Triple Bond. *Nat. Chem.* **2013**, *5*, 1025−1028. (b) Böhnke, J.; Braunschweig, H.; Dellermann, T.; Ewing, W. C.; Hammond, K.; Jimenez-Halla, J. O. C.; Kramer, T.; Mies, J. The Synthesis of $B_2(SIDip)_2$ and its Reactivity Between the Diboracumulenic and Diborynic Extremes. *Angew. Chem., Int. Ed.* **2015**, *54*, 13801−13805. (c) Arrowsmith, M.; Böhnke, J.; Braunschweig, H.; Celik, M. A.; Dellermann, T.; Hammond, K. Uncatalyzed Hydrogenation of First-Row Main Group Multiple Bonds. *Chem. - Eur. J.* **2016**, *22*, 17169−17172. (d) Arrowsmith, M.; Boehnke, J.; Braunschweig, H.; Celik, M. A.; Claes, C.; Ewing, W. C.; Krummenacher, I.; Lubitz, K.; Schneider, C. Neutral Diboron Analogues of Archetypal Aromatic Species by Spontaneous Cycloaddition. *Angew. Chem., Int. Ed.* **2016**, *55*, 11271−11275. (e) Stennett, T. E.; Bertermann, R.; Braunschweig, H. Construction of Linear and Branched Tetraboranes by 1,1- and 1,2-Diboration of Diborenes. *Angew. Chem., Int. Ed.* **2018**, *57*, 15896−15901. (f) Brückner, T.; Dewhurst, R. D.; Dellermann, T.; Müller, M.; Braunschweig, H. Mild Synthesis of Diboryldiborenes by Diboration of B-B Triple Bonds. *Chem. Sci.* **2019**, *10*, 7375−7378. (g) Brückner, T.; Stennett, T. E.; Heß, M.; Braunschweig, H. Single and Double Hydroboration of B-B Triple Bonds and Convergent Routes to a Cationic Tetraborane. *J. Am. Chem. Soc.* **2019**, *141*, 14898−14903. (h) Stennett, T. E.; Jayaraman, A.; Brückner, T.; Schneider, L.; Braunschweig, H. Hydrophosphination of Boron-Boron Multiple Bonds. *Chem. Sci.* **2020**, *11*, 1335−1341.

(4) (a) Power, P. P. Interaction of Multiple Bonded and Unsaturated Heavier Main Group Compounds with Hydrogen, Ammonia, Olefins, and Related Molecules. *Acc. Chem. Res.* **2011**, *44*, 627−637. (b) Hanusch, F.; Groll, L.; Inoue, S. Recent Advances of Group 14 Dimetallenes and Dimetallynes in Bond Activation and Catalysis. *Chem. Sci.* **2021**, DOI: 10.1039/D0SC03192E.

(5) Peng, Y.; Ellis, B. D.; Wang, X.; Fettinger, J. C.; Power, P. P. Reversible σ-Complexation of Ethylene by Main Group Molecules under Ambient Conditions. *Science* **2009**, *325*, 1668−1670.

(6) Wang, S.; Sherbow, T. J.; Berben, L. A.; Power, P. P. Reversible Coordination of H_2 by a Distannyne. *J. Am. Chem. Soc.* **2018**, *140*, 590−593.

(7) Sugahara, T.; Guo, J.-D.; Sasamori, T.; Nagase, S.; Tokitoh, N. Regioselective Cyclotrimerization of Terminal Alkynes Using a Digermyne. *Angew. Chem., Int. Ed.* **2018**, *57*, 3499−3503.

(8) Weetman, C.; Bag, P.; Szilvasi, T.; Jandl, C.; Inoue, S. CO_2 Fixation and Catalytic Reduction by a Neutral Aluminum Double Bond. *Angew. Chem., Int. Ed.* **2019**, *58*, 10961−10965.

(9) Ogawa, T.; Ruddy, A. J.; Sydora, O. L.; Stradiotto, M.; Turculet, L. Cobalt- and Iron-Catalyzed Isomerization-Hydroboration of Branched Alkenes: Terminal Hydroboration with Pinacolborane and 1,3,2-Diazaborolanes. *Organometallics* **2017**, *36*, 417−423.

(10) Arrowsmith, M.; Böhnke, J.; Braunschweig, H.; Deißenberger, A.; Dewhurst, R. D.; Ewing, W. C.; Hörl, C.; Mies, J.; Muessig, J. H. Simple Solution-Phase Syntheses of Tetrahalodiboranes(4) and Their Labile Dimethylsulfide Adducts. *Chem. Commun.* **2017**, *53*, 8265−8267.

(11) Braunschweig, H.; Dewhurst, R. D.; Hammond, K.; Mies, J.; Radacki, K.; Vargas, A. Ambient-Temperature Isolation of a Compound with a Boron-Boron Triple Bond. *Science* **2012**, *336*, 1420−1422.

(12) Braunschweig, H.; Dewhurst, R. D.; Hoerl, C.; Phukan, A. K.; Pinzner, F.; Ullrich, S. Direct Hydroboration of B═B Bonds: A Mild Strategy for the Proliferation of B-B Bonds. *Angew. Chem., Int. Ed.* **2014**, *53*, 3241−3244.

(13) Bissinger, P.; Braunschweig, H.; Damme, A.; Kupfer, T.; Vargas, A. Base-Stabilized Diborenes: Selective Generation and η^2 Side-on Coordination to Silver(I). *Angew. Chem., Int. Ed.* **2012**, *51*, 9931.

(14) Bissinger, P.; Braunschweig, H.; Damme, A.; Hoerl, C.; Krummenacher, I.; Kupfer, T. Boron as a Powerful Reductant: Synthesis of a Stable Boron-Centered Radical-Anion Radical-Cation Pair. *Angew. Chem., Int. Ed.* **2015**, *54*, 359−362.

(15) Braunschweig, H.; Constantinidis, P.; Dellermann, T.; Ewing, W. C.; Fischer, I.; Hess, M.; Knight, F. R.; Rempel, A.; Schneider, C.; Ullrich, S.; Vargas, A.; Woollins, J. D. Highly Strained Heterocycles Constructed from Boron-Boron Multiple Bonds and Heavy Chalcogens. *Angew. Chem., Int. Ed.* **2016**, *55*, 5606−5609.

(16) Braunschweig, H.; Krummenacher, I.; Lichtenberg, C.; Mattock, J. D.; Schaefer, M.; Schmidt, U.; Schneider, C.; Steffenhagen, T.; Ullrich, S.; Vargas, A. Dibora[2]ferrocenophane: A Carbene-Stabilized Diborene in a Strained cis-Configuration. *Angew. Chem., Int. Ed.* **2017**, *56*, 889−892.

(17) Wang, S. R.; Arrowsmith, M.; Boehnke, J.; Braunschweig, H.; Dellermann, T.; Dewhurst, R. D.; Kelch, H.; Krummenacher, I.; Mattock, J. D.; Muessig, J. H.; Thiess, T.; Vargas, A.; Zhang, J. Engineering a Small HOMO-LUMO Gap and Intramolecular C-H Borylation by Diborene/Anthracene Orbital Intercalation. *Angew. Chem., Int. Ed.* **2017**, *56*, 8009−8013.

(18) Stennett, T. E.; Mattock, J. D.; Pentecost, L.; Vargas, A.; Braunschweig, H. Chelated Diborenes and Their Inverse-Electron-Demand Diels-Alder Reactions with Dienes. *Angew. Chem., Int. Ed.* **2018**, *57*, 15276−15281.

(19) Muessig, J. H.; Thaler, M.; Dewhurst, R. D.; Paprocki, V.; Seufert, J.; Mattock, J. D.; Vargas, A.; Braunschweig, H. Phosphine-Stabilized Diiododiborenes: Isolable Diborenes with Six Labile Bonds. *Angew. Chem., Int. Ed.* **2019**, *58*, 4405−4409.

(20) Stennett, T. E.; Bissinger, P.; Griesbeck, S.; Ullrich, S.; Krummenacher, I.; Auth, M.; Sperlich, A.; Stolte, M.; Radacki, K.; Yao, C.-J.; Wuerthner, F.; Steffen, A.; Marder, T. B.; Braunschweig, H. Near-Infrared Quadrupolar Chromophores Combining Three-Coordinate Boron-Based Superdonor and Superacceptor Units. *Angew. Chem., Int. Ed.* **2019**, *58*, 6449−6454.

(21) Bissinger, P.; Braunschweig, H.; Celik, M. A.; Claes, C.; Dewhurst, R. D.; Endres, S.; Kelch, H.; Kramer, T.; Krummenacher, I.; Schneider, C. Synthesis of Cyclic Diborenes with Unprecedented cis-Configuration. *Chem. Commun.* **2015**, *51*, 15917−15920.

(22) Arrowsmith, M.; Boehnke, J.; Braunschweig, H.; Celik, M. A.; Dellermann, T.; Hammond, K. Uncatalyzed Hydrogenation of First-

https://doi.org/10.1021/jacs.0c12627
J. Am. Chem. Soc. 2021, 143, 4993−5002

Row Main Group Multiple Bonds. *Chem. - Eur. J.* **2016**, *22*, 17169−17172.
(23) Auerhammer, D.; Arrowsmith, M.; Bissinger, P.; Braunschweig, H.; Dellermann, T.; Kupfer, T.; Lenczyk, C.; Roy, D. K.; Schaefer, M.; Schneider, C. Increasing the Reactivity of Diborenes: Derivatization of NHC-Supported Dithienyldiborenes with Electron-Donor Groups. *Chem. - Eur. J.* **2018**, *24*, 266−273.
(24) Wang, Y.; Quillian, B.; Wei, P.; Wannere, C. S.; Xie, Y.; King, R. B.; Schaefer, H. F., III; Schleyer, P. V. R.; Robinson, G. H. A Stable, Neutral Diborene Containing a B═B Double Bond. *J. Am. Chem. Soc.* **2007**, *129*, 12412−12413.
(25) Lu, W.; Li, Y.; Ganguly, R.; Kinjo, R. Alkene-Carbene Isomerization Induced by Borane: Access to an Asymmetrical Diborene. *J. Am. Chem. Soc.* **2017**, *139*, 5047−5050.
(26) Stoy, A.; Boehnke, J.; Jimenez-Halla, J. O. C.; Dewhurst, R. D.; Thiess, T.; Braunschweig, H. CO_2 Binding and Splitting by Boron-Boron Multiple Bonds. *Angew. Chem., Int. Ed.* **2018**, *57*, 5947−5951.
(27) (a) Chong, C. C.; Kinjo, R. Catalytic Hydroboration of Carbonyl Derivatives, Imines, and Carbon Dioxide. *ACS Catal.* **2015**, *5*, 3238−3259. (b) Hadlington, T. J.; Kefalidis, C. E.; Maron, L.; Jones, C. Efficient Reduction of Carbon Dioxide to Methanol Equivalents Catalyzed by Two-Coordinate Amido-Germanium(II) and -Tin(II) Hydride Complexes. *ACS Catal.* **2017**, *7*, 1853−1859.
(28) Leong, B.-X.; Teo, Y.-C.; Condamines, C.; Yang, M.-C.; Su, M.-D.; So, C.-W. A NHC-Silyliumylidene Cation for Catalytic N-Formylation of Amines Using Carbon Dioxide. *ACS Catal.* **2020**, *10*, 14824−14833.
(29) Blondiaux, E.; Pouessel, J.; Cantat, T. Carbon Dioxide Reduction to Methylamines under Metal-free Conditions. *Angew. Chem., Int. Ed.* **2014**, *53*, 12186−12190.
(30) Chen, W.-C.; Shen, J.-S.; Jurca, T.; Peng, C.-J.; Lin, Y.-H.; Wang, Y.-P.; Shih, W.-C.; Yap, G. P. A.; Ong, T.-G. Expanding the Ligand Framework Diversity of Carbodicarbenes and Direct Detection of Boron Activation in the Methylation of Amines with CO_2. *Angew. Chem., Int. Ed.* **2015**, *54*, 15207−15212.
(31) Leong, B.-X.; Lee, J.; Li, Y.; Yang, M.-C.; Siu, C.-K.; Su, M.-D.; So, C.-W. A Versatile NHC-Parent Silyliumylidene Cation for Catalytic Chemo- and Regioselective Hydroboration. *J. Am. Chem. Soc.* **2019**, *141*, 17629−17636.

■ NOTE ADDED AFTER ASAP PUBLICATION

After ASAP publication on January 21, 2021, DFT calculations of the catalytic mechanism were revised, as a mechanistic pathway with a lower kinetic barrier was found. The calculations are consistent with experimental observations and do not affect the conclusions in the article. Scheme 6 and the related text have been revised, and DFT data have been added to Tables S19−S24 in the Supporting Information. The corrected version was reposted on March 29, 2021.

https://doi.org/10.1021/jacs.0c12627
J. Am. Chem. Soc. 2021, 143, 4993−5002